Homologous Expression of Lipid Droplet Protein Enhanced Neutral Lipid Accumulation in the Marine Diatom *Phaeodactylum tricornutum*

Kohei Yoneda[1], Masaki Yoshida[2], Iwane Suzuki[2], Makoto M. Watanabe[2]

[1]Graduate School of Life and Environmental Sciences, University of Tsukuba, Ibaraki 305-8572, Japan

[2]Faculty of Life and Environmental Sciences, University of Tsukuba, Ibaraki 305-8572, Japan

Corresponding author: Masaki Yoshida

Faculty of Life and Environmental Sciences, University of Tsukuba, 1-1-1 Tennodai, Tsukuba, Ibaraki 305-8572, Japan

Tel.: +81-29-853-4301; Fax: +81-29-853-4301; E-mail: yoshida.masaki.gb@u.tsukuba.ac.jp

Abstract

Lipid droplets are ubiquitous cellular compartments that store neutral lipids and specific proteins localize on their surface. These proteins work as a scaffold in maintaining the lipid droplet structure or as regulators of lipogenesis or lipolysis. Previously, our group was the first to identify the most abundant lipid droplet protein, namely stramenopile-type lipid droplet protein (StLDP), in the marine diatom *Phaeodactylum tricornutum*; however, its function remains unclear because StLDP does not reveal homology with known lipid droplet proteins and lacks a predictable domain. In this study, we transformed *P. tricornutum* to express a homologous StLDP gene under an fcpA promoter in order to determine its function. StLDP expression was strongly enhanced in the mutant (H8), especially in nitrogen-sufficient conditions; however, it was attenuated in nitrogen-deficient conditions. Despite the strong expression, no significant difference was observed in the lipid composition between the wild type (WT) and H8 under nitrogen-sufficient conditions. After cultivation in nitrogen-free medium for 6 days, neutral lipid content significantly increased in H8 than in WT. After 2 days of cultivation in nitrogen-free medium, 97.0% of single cells in WT formed one or two lipid droplets, whereas in H8, this proportion decreased to 78.8%, and the proportion of cells forming three or four lipid droplets increased. Thus, we speculate that StLDP functions to sequester triacylglycerol on the initial lipid droplet formation.

Keywords

Nitrogen starvation, Overexpression, StLDP, Triacylglycerol

Introduction

Microalgal biomass has attracted immense attention as a candidate biodiesel feedstock due to an increasing interest in the production of renewable feedstock to protect the global environment and to develop a sustainable society (Huang et al. 2010, Mata et al. 2010). Microalgae can produce several metabolites through photosynthesis using light energy and carbon dioxide (Mata et al. 2010). The marine diatom, *Phaeodactylum tricornutum*, is one of the most promising microalgae for biomass production. It grows faster and can accumulate 20–30% oils (Chisti 2007), which can be used as a feedstock for biodiesel or dietary supplements containing polyunsaturated fatty acid, eicosapentaenoic acid (Fajardo et al. 2007). Similar to other microalgae, the lipid content of *P. tricornutum* increases under nitrogen deficiency (Abida et al. 2015). Herein, *P. tricornutum* forms oil-rich cellular compartments called lipid droplets (Guiheneuf et al. 2011). The chief constituent of lipid droplets in *P. tricornutum* is triacylglycerol (TAG) (Yoneda et al. 2016). Not only microalgae but also various organisms including mammals, fruits flies, yeast, bacteria, land plants possess lipid droplets (Murphy and Bance 1999, Murphy 2012); there are thought to be generated from the phospholipid bilayer of the endoplasmic reticulum (ER), and certain proteins are found to localize on the droplet surface (Ohsaki et al. 2014). Some of these proteins function as a scaffold for the lipid droplet in maintaining the globule size, whereas the other proteins reveal diverse functions in lipid metabolism (lipogenesis and lipolysis), cellular signaling, or membrane trafficking (Martin and Parton 2006, Pol et al. 2014).

Proteomic analyses of fractionated lipid droplets have identified the proteins present on these lipid droplets in many organisms (Yang et al. 2012). The perilipin (Plin) and oleosin families of proteins are found as the major proteins on the lipid

droplets in mammalian tissues and seed cells of spermatophytes, respectively (Yang et al. 2012). At present, five proteins belong to the Plin protein family (Plin1–5) (Kimmel et al. 2010). Plin1 and Plin4 are mainly distributed in the adipose tissue, Plin2 and Plin3 are ubiquitously expressed in the tissues possessing lipid droplets, and Plin5 is expressed in the oxidative tissues such as heart muscle (Sztalryd and Kimmel 2014). Plin1 and Plin2 are the most abundant proteins of cytosolic lipid droplets in the adipose tissue and the liver, respectively (Sztalryd and Kimmel 2014). The oleosin family comprises three proteins: oleosin, caleosin, and steroleosin (Chapman et al. 2012). Oleosin is a major coat protein on the lipid droplets in seed cells. In the microalgal lipid droplets, homologs of the major lipid droplet protein (MLDP) were found in the green algae *Chlamydomonas reinhardtii* (Moellering and Benning 2010, Nguyen et al. 2011), *Dunaliella salina* (Davidi et al. 2012), and *Lobosphera incisa* (Siegler et al. 2017) through proteomic analysis, and in *Scenedesmus quadricauda* using immunology (Javee et al. 2016). In addition, *Haematococcus* oil globule protein (HOGP), an ortholog of MLDP, was found in the green algae, *Haematococcus pluvialis* (Peled et al. 2011). Moreover, lipid droplet proteomics were conducted in the green algae, *Chlorella* sp. (Lin et al. 2012), endosymbiotic dinoflagellates *Symbiodinium* (Pasaribu et al. 2014), haptophytes *Tisochrysis lutea* (Shi et al. 2015), eustigmatophytes *Nannochloropsis oceanica* (Vieler et al. 2012), and the diatom *Fistulifera* sp. JPCC DA0580 (Nojima et al. 2013). Initially, we performed proteomic analysis on the lipid droplets isolated from *P. tricornutum* and identified a new lipid droplet protein, namely stramenopile-type lipid droplet protein (StLDP) (Yoneda et al. 2016). Although StLDP was identified as the main protein of the lipid droplets in *P. tricornutum*, its function remains unclear because StLDP does not reveal homology with other known lipid droplet proteins and

lacks a predictable catalytic domain.

According to reports on modifying the expression levels of main lipid droplet protein, the upregulation of gene expression led to fat accumulation in certain cases. For example, the adenoviral overexpression of Plin2, a major lipid-droplet-coating protein in liver, caused hepatosteatosis in mice, and the TAG content increased two-fold higher in the liver steatosis tissue when compared with the control (Sun et al. 2012). Increasing TAG amounts and dysfunctional effects were also observed with Plin5 overexpression in the mouse cardiomyocytes (Pollak et al. 2013, Wang et al. 2013). Alternatively, the overexpression of Plin1, a major lipid-droplet-coating protein in the adipose tissue, led to a leaner phenotype and lower adipose depot weight in the transgenic mice when compared with the wild type (WT) mice (Miyoshi et al. 2010).

In a land plant study, Liu et al. (2013) reported that the transgenic rice seeds expressing soybean oleosin exhibited around 1.4-fold higher lipid content than WT; however, the detailed mechanisms facilitating lipid accumulation still remain unclear. Heterologous expression of Plin and oleosin in the yeast, *Saccharomyces cerevisiae*, elevated the neutral lipid levels under radiolabeled palmitic acid feeding conditions (Jacquier et al. 2013). Shemesh et al. (2016) also performed heterologous expression of the green algal HOGP gene in *P. tricornutum* and reported higher total fatty acid content and TAG accumulation. To the best of our knowledge, no reports are available on the homologous expression of the main lipid droplet protein in microalgae.

In this study, we produced a *P. tricornutum* mutant with an enhanced expression of homologous StLDP gene to determine the function of the lipid droplet protein, and hypothesized that it would facilitate lipid accumulation.

Materials and methods

Microalgal strain and culture conditions

P. tricornutum CCAP1052/6 was cultivated at 20 °C with continuous light at 70 µmol photons m^{-2} s^{-1}. Half strength seawater, prepared using 17 gL^{-1} of Coral Pro salt (Red Sea, Eilat, Israel) and enriched with f/2 nutrient (Guillard and Ryther 1962), was used for the strain maintenance and during the course of transformation. 4f medium containing 8-fold higher nitrate and phosphate concentrations than in f/2 was used in the main cultivation experiment. We performed the main cultivation in 200 mL Erlenmeyer flasks with 120 mL liquid medium, and ambient air was bubbled for agitation.

Construction of plasmids

For the expression of StLDP-enhanced green fluorescent protein (EGFP) fusion protein and histidine-tagged (his-tag) StLDP in *P. tricornutum*, we constructed two plasmids: pPT-FP and pPT-StLDP-his. The pPT-FP plasmid contained the expression cassette of the fusion gene comprising EGFP gene fused to the C-terminal of the StLDP gene from *P. tricornutum*. We deleted the stop codon from StLDP and the start codon from EGFP and connected them with glycine linker (×5 glycine). The pPT-StLDP-his plasmid comprised StLDP gene with six additional histidines at the C-terminal.

The pPha-T1 plasmid reported by Zaslavskaia et al. (2000) was used as the backbone of both expression plasmids. The multicloning site (MCS) of the pPha-T1 was located between the fucoxanthin–chlorophyll binding protein (fcp) A promoter and terminator. Thus, the inserted gene in the MCS was expressed under the control

of the fcpA promoter. In addition, pPha-T1 contained a *sh ble* gene expression cassette to confer zeosin resistance. The pPha-T1 and pPTEGfp plasmids comprising the EGFP gene in the pPha-T1 plasmid (Zaslavskaia et al. 2000) were a kind gift from Prof. Peter Kroth, University of Konstanz. The primers used in this study are summarized in Table S1.

For the constructing pPT-FP, DNA fragments of StLDP and EGFP were individually amplified from the genomic DNA of *P. tricornutum* and pPTEGfp by polymerase chain reaction (PCR) using the primer sets LD_F/FP-LD_R and FP-EGFP_F/EGFP_R, respectively. Both fragments were then mixed and fused using PCR. The fused PCR product was double-digested by EcoRI and HindIII, and was inserted into the corresponding cloning site in the pPha-T1 with DNA Ligation Kit, Mighty Mix (Takara Bio, Otsu, Japan).

For constructing pPT-StLDP-his, DNA fragment of StLDP was amplified from genomic DNA by PCR using a LD_F/LD-His_R primer set. The PCR product was then inserted into the EcoRI/HindIII sites in the pPha-T1 plasmid in similar manner.

Eventually, we confirmed the DNA sequences of the inserted genes in the plasmids by DNA sequencing using a BigDye Cycle Sequencing Kit (Thermo Fisher Scientific, Boston, MA, USA) and a 3130 Genetic Analyzer (Applied Biosystems, Carlsbad, CA, USA).

Transformation of diatoms

The diatom cells were transformed using the protocol described by Zaslavskaia et al. (2000) with minor modifications. Approximately 7×10^7 cells were spread on an agar plate and bombarded using a BioRad Biolistic PDS-1000/He Particle Delivery System (BioRad, Hercules, CA, USA) with a 1350 psi rupture disc. Gold particles (1.0 μm

diameter) that coated with 3 μg of circular plasmid DNA, 0.1 M spermidine, and 2.5 M $CaCl_2$ were bombarded twice per plate. After an overnight recovery culture, the bombarded diatom cells were then cultivated on a selection plate containing 50 μg mL^{-1} zeocin. Gene integration into the genomic DNA was confirmed by PCR using the specific primers for the his-tag StLDP (LD_F/6His-spe_R) and StLDP-EGFP (LD_F/EGFP_R).

Microscopic observation of the localization of the StLDP-EGFP fusion protein

We cultivated the mutants in f/2 medium under static conditions as described elsewhere and microscopic images were captured using an Olympus BX53 microscope system (Olympus, Center Valley, PA, USA) equipped with a BNA fluorescent mirror (green filter; excitation, 475–495 nm, absorption, 510–550 nm).

Cultivation experiment in nitrogen-deficient medium

WT and his-tagged StLDP-expressing strains (His1-22-8; H8) were precultured in 4f medium for 1 week and were inoculated in fresh 4f medium. The initial cell concentrations were adjusted to 0.15 at an optical density of 750 nm. The strains were cultivated in nitrogen-sufficient medium for 4 days, and were then transferred to nitrogen-deficient 4f medium that lacked a nitrogen source. Before the transfer, we washed the cells twice with nitrogen-deficient medium. Cultivation under nitrogen-deficient conditions lasted for 6 days.

Dry cell weight (DCW) measurement and lipid analysis

For DCW measurements, cells in 10 mL culture broth were harvested on the preweighted GF/C glass filter, and were dried at 55 °C in an oven. The dried biomass

196 residues on the filter were then gravimetrically measured.

197 We extracted crude lipids using Folch method (Folch et al. 1957). The wet
198 biomass pellet obtained by centrifugation of 50 mL of culture broth was used directly
199 for chloroform/methanol extraction. The amount of the crude lipid extracts was
200 measured gravimetrically after the extraction. The composition of neutral and polar
201 lipids was determined using silica gel column chromatography with Silica Gel 60
202 (Merck, Darmstadt, Germany) as a support. The crude lipids were eluted first using
203 chloroform (four times the volume of the column bed), followed by the same volume
204 of methanol. The chloroform fraction contained neutral lipids, mainly TAG, whereas
205 the methanol fraction contained polar lipids such as phospholipids and glycolipids.

206

207 **RNA extraction and qRT–PCR**

208 The RNA extraction procedure and qRT–PCR for the quantification of StLDP
209 expression were performed as per our previous report (Yoneda et al. 2016). In this
210 study, we used TRIzol reagent (Thermo Fisher Scientific, Boston, MA, USA) and
211 RNeasy Mini Kit (Qiagen, Hilden, Germany) for total RNA extraction. A PrimeScript
212 RT Reagent Kit with gDNA Eraser (Takara Bio, Shiga, Japan) was used to eliminate
213 residual genomic DNA and cDNA synthesis, and SYBR Premix ExTaq II (Tli RNaseH
214 Plus) (Takara Bio, Shiga, Japan) was used for the two-step real-time qRT–PCR.

215

216 **Quantification of lipid droplet size and number**

217 Lipid droplet were stained with Nile red (Wako, Osaka, Japan) and were observed
218 under fluorescent microscopy. The captured images were analyzed using ImageJ
219 (Abramoff et al. 2004). The dots derived from the Nile red-stained lipid droplets were
220 numbered and the size of each fluorescent area was measured using the ImageJ.

The diameters of the lipid droplets were calculated from the area, and the numbers of lipid droplets per cell were manually enumerated from the processed images.

Results

Localization of StLDP–EGFP fusion protein

We previously identified StLDP from the lipid droplet fraction obtained from *P. tricornutum* (Yoneda et al. 2016); however, we did not confirm the localization of StLDP. Therefore, we attempted to express the StLDP–EGFP fusion protein in *P. tricornutum*. Figure 1 presents the subcellular localization of EGFP and the StLDP–EGFP fusion protein. EGFP fluorescence was broadly observed in the cell (Fig. 1A), whereas the green fluorescence from the fusion protein (StLDP–EGFP) was localized at the lipid droplet in *P. tricornutum* (Fig. 1B). Thus, StLDP was confirmed as a lipid droplet protein in *P. tricornutum*.

Growth curve, DCW, lipid content, and expression levels of StLDP in WT and mutant

To determine the function of StLDP, WT and his-tagged StLDP-expressing strain (H8) were cultivated in nitrogen-sufficient medium for 4 days and in nitrogen-deficient medium for 6 days. Figure 2A presents the growth curve of these strains and Figure 2B reveals the DCW and lipid amounts at the end of cultivation (Day 10). No significant differences were seen in the growth, DCW, or crude lipid amounts between the strains. Figure 2C represents the expression levels of StLDP at Days 4, 7, and 10. StLDP expression in H8 was 57-fold higher than that in WT at Day 4; however, the enhanced StLDP expression in H8 decreased at Day 7 to a level that was 1.2-fold higher than the WT, and finally reached the same level as the WT at Day 10. Gene

246 expression of the introduced his-tagged StLDP under the control of fcpA promoter
247 was attenuated after the prolonged cultivation period under nitrogen starvation.
248
249 **Lipid composition in WT and mutant**
250 Figure 3 indicates the proportion of neutral and polar lipids in WT and H8 mutant at
251 Days 4 and 10. The composition of neutral lipids in the crude lipid was similar in both
252 strains at Day 4 (33.2 ± 1.3% and 33.4 ± 1.4% in WT and H8, respectively; Fig. 3A). A
253 significant increase in the percentage composition of neutral lipid was observed at
254 Day 10 (45.3 ± 2.8% and 53.5 ± 2.3% in WT and H8, respectively; Fig. 3B; P = 0.007,
255 Student's t-test, n = 3). On the contrarily, the percentage composition of the polar
256 lipids significantly decreased in the H8 mutant when compared with WT (Fig. 3B; P =
257 0.035, Student's t-test, n = 3). When we converted the crude lipids to DCW, a
258 significant increase in the neutral lipid content was observed in the H8 mutant (Fig.
259 3C; P = 0.026, Student's t-test, n = 3). This suggested that the homologous
260 expression of StLDP promoted the accumulation of neutral lipid.
261
262 **Microscopic observation during cultivation in nitrogen-deficient medium**
263 Figure 4 presents the microscopic images of WT and H8 mutant at Days 4, 6, and 10.
264 At Day 4, just before inoculation into the nitrogen-deficient medium, none of strains
265 formed lipid droplets in the cells (Fig. 4A). This observation revealed that the
266 overexpression of StLDP per se did not trigger the formation of lipid droplets. Even at
267 Day 5, scanty lipid droplets were seen; however, after Day 6, the lipid droplets were
268 observed in WT and H8 mutant (Fig. 4B), revealing that the timing of induction of lipid
269 droplet formation was same in both strains. At the end of cultivation (Day 10), we
270 could observe larger lipid droplets in H8 than WT (Fig. 4C), suggesting that lipid

droplet fused with each other as the result of attenuation of StLDP expression in the H8 strain under prolonged cultivation period under nitrogen starvation.

Lipid droplet diameter and the number of lipid droplets per cell

As shown in Figure 3 (B, C), the neutral lipid composition increased in the H8 mutant at the final day (Day 10). The expression level of StLDP was strongly enhanced in the H8 mutant at Day 4, prior to cultivation in the nitrogen-deficient medium (Fig. 2C); however, neutral lipid accumulation and lipid droplet formation was not observed at the Day 4 (Figs. 3A and 4A). Thus, the major effects of the StLDP expression occurred after reinoculation into the nitrogen-deficient medium. We speculated that the major effect was occurred at the initial stage of nitrogen deprivation because the expression of introduced his-tagged StLDP decreased to the same level as the WT at later stages (Day 10, Fig. 2C). Herein, we focused on the size and number of lipid droplets, especially at Day 6, the initial stage of lipid droplet formation.

Figure 5 (A, B) presents the distribution of the diameter of each lipid droplet at Days 6 and 10. At Day 6, the distribution of the lipid droplet diameter was similar in the WT and H8 mutant (Fig. 5A), and the average diameter did not differ either of the strains (1.26 ± 0.47 μm and 1.36 ± 0.52 μm in WT and H8, respectively). Alternatively, the proportion of larger lipid droplet increased in H8 mutant at Day 10 (Fig. 5B) and reflected higher neutral lipid content in H8 mutant at Day 10 (Fig. 3B). Figure 5C reveals the number of lipid droplets per cell at Day 6. In WT, almost all single cells (97.0%) formed one or two lipid droplet(s), whereas in the H8 mutant, the proportion decreased to 78.8% and the proportion of the cells that formed three or four lipid droplets was increased (15.1 and 6.0%, respectively; Fig. 5C). In particular, on the size distribution, the lipid droplets were similar; however, the number of lipid droplets

per cell changed between the strains at Day 6. These observation suggested that the enhanced StLDP expression increased the number of lipid droplets per cell at the initial nitrogen-deficient period and led to the promotion of the neutral lipid accumulation.

Discussion

Growth and expression levels of StLDP in mutant

As shown in Figure 2A, the expression of his-tagged StLDP in the H8 mutant did not lead to growth inhibition; however, overexpression of StLDP in the H8 mutant was restricted on Day 4 (Fig. 2C). This was explained by the attenuation of expression by the fcpA promoter under nitrogen deficiency. A transcriptomic study of *P. tricornutum* demonstrated that the LHCF1 gene (also known as fcpA) and several genes related to the photosynthesis and pigment biosynthesis were repressed during nitrogen deprivation (Alipanah et al. 2015). To improve the expression levels under nitrogen deprivation, Shemesh et al. (2016) developed a new promoter of the DGAT1 gene in *P. tricornutum*; however, they reported that although pDGAT1 promoted gene expression under nitrogen deprivation, the expression levels were still lower than the other promoters (e.g., fcpA). Utilization of pDGAT1 or other promoters that express under nitrogen deprivation requires for further investigation.

Accumulation of neutral lipids in nitrogen-deficient conditions and function of StLDP

Despite the restriction of overexpression by the fcpA promoter, significant differences were observed in the lipid composition (Fig. 3). In this study, the percentage neutral lipid content was increased by 18% in the H8 mutant when compared with WT (Fig.

3B). Elevation of neutral lipid due to the expression of lipid droplet proteins has often been reported in previous studies (Sun et al. 2012, Pollak et al. 2013, Wang et al. 2013). Lipid droplet-coating proteins likely function to protect stored lipid (i.e., TAG) from cytosolic lipases. Thus, one of the reasons for oil accumulation induced by StLDP overexpression could be due to the enhanced protection ability and the interruption of hydrolyzes by the lipases (Miyoshi et al. 2010, Pollak et al. 2013).

In transgenic mice, the overexpression of Plin1 led to a leaner phenotype and lower fat accumulation in the adipocytes. This was explained by the differentiation of white adipose tissue to a more energy-consuming brown adipose-like tissue that led to higher energy expenditure, upregulation of mitochondrial fatty acid β-oxidation, and downregulation of lipogenic genes (Sawada et al. 2010, Miyoshi et al. 2010). Alternatively, the overexpression of Plin5 in mouse heart tissue slightly downregulated the mitochondrial medium chain acyl-CoA dehydrogenase that is related to fatty acid β-oxidation (Wang et al. 2013). It is likely that StLDP linked to the lipogenic or lipolytic pathways especially under nitrogen deficiency. Alternatively, it is not likely in nitrogen-sufficient conditions because the lipid composition in the H8 mutant did not differ from WT in the nitrogen-sufficient conditions (Fig. 3A).

According to Jacquier et al. (2013), heterologous expression of Plin family proteins and oleosin in the yeast, *S. cerevisiae*, led to increased TAG levels. Deletion mutants of phosphatidate phosphatase, PAH1, which catalyzes the dephosphorylation of phosphatidate during the glycerolipid biosynthesis, could not form lipid droplets in the cell, and TAG and sterol ester (STE) existed at the bilayer of ER membrane in the *pah1Δ* yeast mutant (Jacquier et al. 2013). Irregular accumulation of neutral lipids on the ER membrane is unfavorable for ER-localizing lipogenic enzymes as it changes the physical properties of the ER membrane and the

products remain at the reaction site. The expression of Plins and oleosin in the *pah1Δ* mutant led to the relocation of these neutral lipids into the lipid droplet and the enhanced TAG and STE biosynthesis (Jacquier et al. 2013). The authors concluded that the accumulated neutral lipids on the ER membrane were released by the expression of Plin and oleosin that facilitated the sequestration of synthesized neutral lipid product (i.e., TAG and STE) from the ER to the lipid droplet. In our study, after cultivation in the nitrogen-deficient medium, the percentage composition of neutral lipid was increased in the H8 mutant (Fig. 3C), and the proportion of cells that had more than three lipid droplets in a single cell at Day 6 was increased in the H8 mutant (Fig. 5C). Thus, we hypothesized that StLDP facilitated the sequestration of TAG at the initial stage of lipid droplet formation and led to an increase in the number of lipid droplets in the H8 mutant. At the end of the cultivation (Day 10), the proportion of large lipid droplets increased in the H8 mutant (Fig. 5B). We speculated that tiny lipid droplets generated at Day 6 fused with each other due to a decrease in coating protein caused by the attenuation of StLDP expression during nitrogen deficiency (Fig. 2C), producing large lipid droplets observed at Day 10 in the H8 mutant. Prolonged upregulation of the StLDP gene in the nitrogen-deficient culture may enhance further lipid accumulation through the physical barrier effects of lipid-droplet-coating proteins. Further studies are necessary to determine whether StLDP is involved in the regulation of lipogenic or lipolytic enzymes in the nitrogen-deficient conditions.

Acknowledgments

This study was supported by the Grant-in-Aid for Japan Society for the Promotion of Science (JSPS) Research Fellow [JSPS KAKENHI Grant Number JP17J03747 to

K.Y.].

Compliance with Ethical Standards

The authors declare no conflicts of interest.

References

Abida H, Dolch LJ, Meï C, Villanova V, Conte M, Block MA, Finazzi G, Bastien O, Tirichine L, Bowler C, Rébeillé F (2015) Membrane glycerolipid remodeling triggered by nitrogen and phosphorus starvation in *Phaeodactylum tricornutum*. Plant Physiol 167: 118-136.

Abramoff MD, Magalhaes PJ, Ram SJ (2004) Image processing with Image. J Biophotonical International 11: 36-42.

Alipanah L, Rohloff J, Winge P, Bones AM, Brembu T (2015) Whole-cell response to nitrogen deprivation in the diatom *Phaeodactylum tricornutum.* J. Exp Bot 66: 6281-6296.

Chapman KD, Dyer JM, Mullen RT (2012) Biogenesis and functions of lipid droplets in plants. J Lipid Res 53: 215-216.

Chisti Y (2007) Biodiesel from microalgae. Biotechnol Adv 25: 294-306.

Davidi L, Katz A, Pick U (2012) Characterization of major lipid droplet proteins from *Dunaliella*. Planta 236: 19-33.

Fajardo AR, Cerdan LE, Medina AR, Fermamdez FGA, Moreno PAG, Grima EM (2007) Lipid extraction from the microalga *Phaeodactylum tricornutum*. Eur J Lipid Sci Technol 109: 120-126.

Folch J, Lee M, Stanley GHS (1957) A simple method for the isolation and purification of total lipids from animal tissues. J Biol Chem 226: 497-509.

Guiheneuf F, Leu S, Zarka A, Khozin-Goldberg I, Khalilov I,Boussiba S (2011) Cloning and molecular characterization of a novel acyl-CoA: diacylglycerol acyltransferase 1-like gene (PtDGAT1) from the diatom *Phaeodactylum tricornutum*. FEBS J 278: 3651-3666.

Guillard RRL, Ryther JH (1962) Studies of marine planktonic diatoms. I. *Cyclotella nana* Hustedt and *Detonula confervaceae* (Cleve) Gran. Can J Microbiol 8: 229-239

Huang G, Chen F, Wei D, Zhang X, Chen G (2010) Biodiesel production by microalgal biotechnology. Appl Energ 87: 38-46.

Jacquier N, Mishra S, Choudhary V, Schneiter R (2013) Expression of oleosin and perilipins in yeast promotes formation of lipid droplets from the endoplasmic reticulum. J Cell Sci 126: 5198-5209.

Javee A, Sulochana SB, Pallissery SJ, Arumugam M (2016) Major lipid body protein: A conserved structural component of lipid body accumulated during abiotic stress in *S. quadricauda* CASA-CC302. Front Energ Res 4: 37.

Kimmel AR, Brasaemle DL, McAndrews-Hill M, Sztalryd C, Londos C (2009) Adoption of PERILIPIN as a unifying nomenclature for the mammalian PAT-family of intracellular lipid storage droplet proteins. J Lipid Res 51: 468-471.

Lin I, Jiang P, Chen C, Tzen JTC (2012) A unique caleosin serving as the major integral protein in oil bodies isolated from *Chlorella* sp. cells cultured with limited nitrogen. Plant Physiol Biochem 61:80-87.

Liu WX, Liu HL, Qu LQ (2013) Embryo-specific expression of soybean oleosin altered oil body morphogenesis and increased lipid content in transgenic rice seeds. Theor Appl Genet 126: 2289-2297.

Martin S, Parton RG (2006) Lipid droplets: a unified view of a dynamic organelle. Nat Rev Mol Cell Bio 7: 373-378.

Mata TM, Martins AA, Caetano NS (2010) Microalgae for biodiesel production and other applications: A review. Renew Sust Energ Rev 14: 217-232.

Miyoshi H, Souza SC, Endo M, Sawada T, Perfield JW, Shimizu C, Stancheva Z, Nagai S, Strissel KJ, Yoshioka N, Obin MS (2010) Perilipin overexpression in mice protects against diet-induced obesity. J Lipid Res 51: 975-982.

Moellering ER, Benning C (2010) RNA interference silencing of a major lipid droplet protein affects lipid droplet size in *Chlamydomonas reinhardtii*. Eukaryot Cell 9: 97-106.

Murphy DJ, Vance J (1999) Mechanisms of lipid-body formation. Trends Biochem Sci 24: 109-115.

Murphy DJ (2012) The dynamic roles of intracellular lipid droplets: from archaea to mammals. Protoplasma 249: 541-585.

Nguyen HM, Baudet M, Cuine S, Adriano JM, Barthe D, Billon E, Bruley C, Beisson F, Peltier G, Ferro M, Li-Beisson Y (2011) Proteomic profiling of oil bodies isolated from the unicellular green microalga *Chlamydomonas reinhardtii*: With focus on proteins involved in lipid metabolism. Proteomics 11: 4266-4273.

Nojima D, Yoshino T, Maeda Y, Tanaka M, Nemoto M, Tanaka T (2013) Proteomics analysis of oil body associated proteins in the oleaginous diatom. J Proteome Res12: 5293-5301.

Ohsaki Y, Suzuki M, Fujimoto T (2014) Open questions in lipid droplet biology. Chem Biol 21: 86-96.

Pasaribu B, Lin IP, Tzen JT, Jauh GY, Fan TY, Ju YM, Cheng JO, Chen CS, Jiang PL (2014) SLDP: a novel protein related to caleosin is associated with the endosymbiotic *Symbiodinium* lipid droplets from *Euphyllia glabrescens*. Mar Biotechnol 16: 560-571.

Peled E, Leu S, Zarka A, Weiss M, Pick U, Khozin-Goldberg I, Boussiba S (2011) Isolation of a novel oil globule protein from the green alga *Haematococcus pluvialis* (Chlorophyceae). Lipids 46: 851-861.

Pol A, Gross SP, Parton RG (2014) Biogenesis of the multifunctional lipid droplet:

Lipids, proteins, and sites. J Cell Biol 204: 635-646.

Pollak NM, Schweiger M, Jaeger D, Kolb D, Kumari M, Schreiber R, Kolleritsch S, Markolin P, Grabner GF, Heier C, Zierler KA (2013) Cardiac-specific overexpression of perilipin 5 provokes severe cardiac steatosis via the formation of a lipolytic barrier. J Lipid Res 54: 1092-1102.

Sawada T, Miyoshi H, Shimada K, Suzuki A, Okamatsu-Ogura Y, Perfield II JW, Kondo T, Nagai S, Shimizu C, Yoshioka N, Greenberg AS. (2010) Perilipin overexpression in white adipose tissue induces a brown fat-like phenotype. PLoS ONE 5: e14006.

Shemesh Z, Leu S, Khozin-Goldberg I, Didi-Cohen S, Zarka A, Boussiba S (2016) Inducible expression of Haematococcus oil globule protein in the diatom Phaeodactylum tricornutum: Association with lipid droplets and enhancement of TAG accumulation under nitrogen starvation. Algal Res 18: 321-331.

Shi Q, Araie H, Bakku, RK, Fukao Y, Rakwal R, Suzuki I, Shiraiwa Y (2015) Proteomic analysis of lipid body from the alkenone-producing marine haptophyte alga *Tisochrysis lutea*. Proteomics 15: 4145-4158.

Sun Z, Miller RA, Patel RT, Chen J, Dhir R, Wang H, Zhang D, Graham MJ, Unterman TG, Shulman GI, Sztalryd C (2012) Hepatic Hdac3 promotes gluconeogenesis by repressing lipid synthesis and sequestration. Nat. Med. 18: 934-942.

Sztalryd C, Kimmel AR (2014) Perilipins: Lipid droplet coat proteins adapted for tissue-specific energy storage and utilization, and lipid cytoprotection. Biochimie 96: 96-101.

Vieler A, Brubaker SB, Vick B, Benning C (2012) A Lipid droplet protein on *Nannochloropsis* with functions partially analogous to plant oleosins. Plant Physiol 158: 1562-1569.

Wang H, Sreenivasan U, Gong DW, O'Connell KA, Dabkowski ER, Hecker PA, Ionica N, Konig M, Mahurkar A, Sun Y, Stanley WC (2013) Cardiomyocyte-specific perilipin 5 overexpression leads to myocardial steatosis and modest cardiac dysfunction. J Lipid Res 54: 953-965.

Yang L, Ding Y, Chen Y, Zhang S, Huo C, Wang Y, Yu J, Zhang P, Na H, Zhang H, Ma Y (2012) The proteomics of lipid droplets: structure, dynamics, and functions of organelle conserved from bacteria to humans. J Lipid Res 53: 1245-1253.

Yoneda K, Yoshida M, Suzuki I, Watanabe MM (2016) Identification of a major lipid droplet protein in a marine diatom *Phaeodactylum tricornutum*. Plant Cell Physiol 57: 397-406.

Zaslavskaia LA, Lippmeier JC, Kroth PG, Grossman AR, Apt KE (2000) Transformation of the diatom *Phaeodactylum tricornutum* (Bacillariophyceae) with a variety of selectable marker and reporter genes. J Phycol 36: 379-386.

Figure legends

Figure 1. Subcellular localization of StLDP–EGFP fusion protein.

Microscopic images of EGFP-expressing mutant (A) and StLDP–EGFP fusion protein-expressing mutant (B).

Figure 2. Growth curve, dry cell weight (DCW) and crude lipid amount, and expression levels of StLDP.

(A). Growth curve of wild type (WT) and StLDP-expressing mutant (H8). The cells were cultivated in the nitrogen-sufficient medium for 4 days, and then in the nitrogen-deficient medium for 6 days. Open circles indicate WT and open squares indicate H8 mutant. Values are shown as mean OD_{750} ± SD (*n* = 3). (B). DCW and crude lipid amount at the end of cultivation in WT and H8. (C). Relative expression of StLDP measured by real-time qRT-PCR. Expression levels were measured in samples on the initial day of reinoculation into the nitrogen-deficient medium (Day 4), and then after 3 and 6 days of cultivation in the nitrogen-deficient medium (Days 7 and 10, respectively). Expression levels in WT at Day 4 were considered as 1 (standard) and relative expression levels were calculated. Error bars indicate SD (*n* = 3). Actin12 was used as a housekeeping gene for normalization.

Figure 3. Proportion of neutral and polar lipid in the crude lipid extract of WT and H8 mutant.

Neutral and polar lipid composition in WT and H8 mutant at Day 4 (A) and at Day 10 (B).

Error bars indicate SD, and statistical analyses were performed using Student’s t-test

(*P < 0.05, **P < 0.01, n = 3, one-tailed).

Figure 4. Microscopic images of lipid droplet formation in WT and H8 mutant.
Nile-red stained cells at Day 4 (A), Day 6 (B), and at Day 10 (C). Fluorescent images were captured through a BNA green filter. Lipid droplets containing neutral lipid were visualized as green with the BNA filter. Scale bars represent 10 μm.

Figure 5. Distribution of the diameter of respective lipid droplets and the number of lipid droplets in single cells.
Size distribution of lipid droplets at Day 6 (A) (WT, n = 128; H8, n = 151) and at Day 10 (B) (WT, n = 268; H8, n = 350). Each droplet size was measured using ImageJ. (C). The number of lipid droplets per cell at Day 6 (WT, n = 99; H8, n = 66).

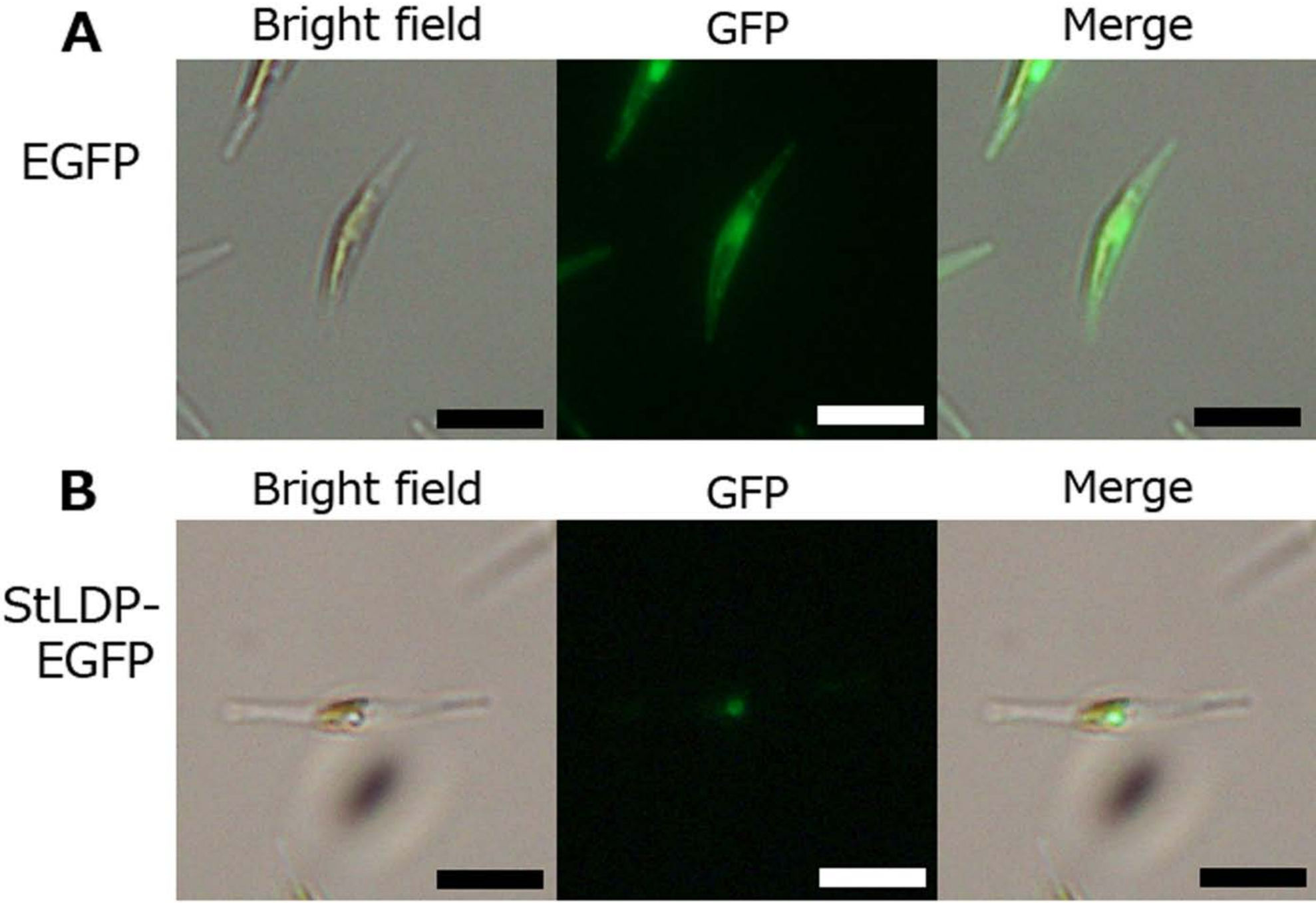
A
Bright field
GFP
Merge
EGFP
B
Bright field
GFP
Merge
StLDP-
EGFP

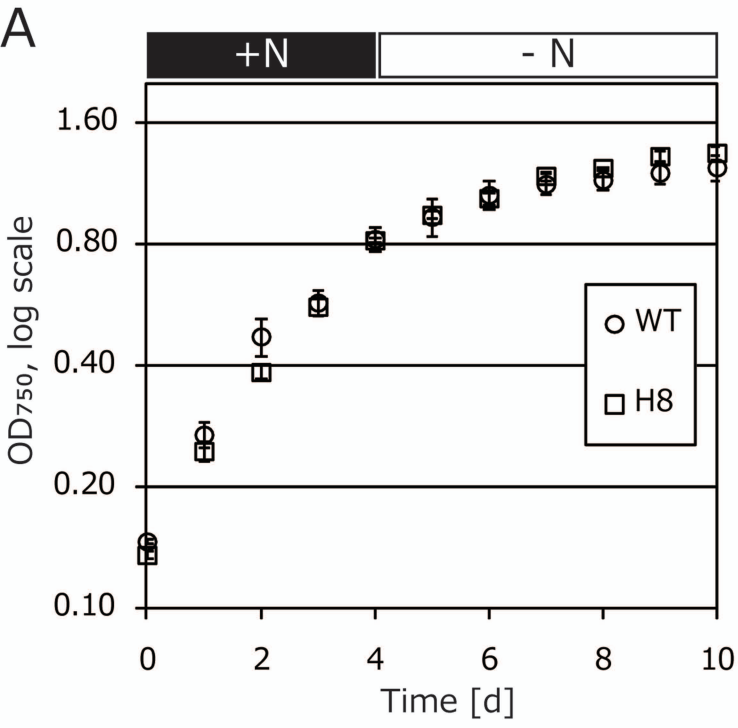
A
+N
- N
1.60
0.80
0.40
0.20
0.10
OD750, log scale
WT
H8
0
2
4
6
8
10
Time [d]

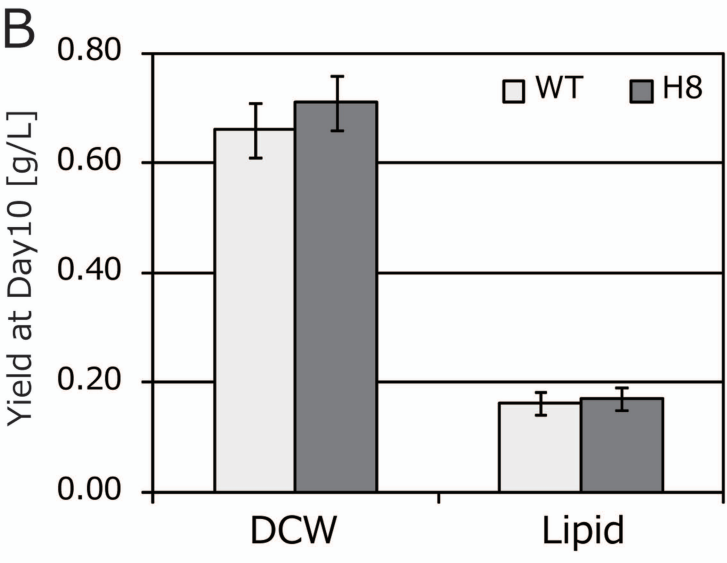
B
0.80
0.60
0.40
0.20
0.00
Yield at Day10 [g/L]
WT
H8
DCW
Lipid

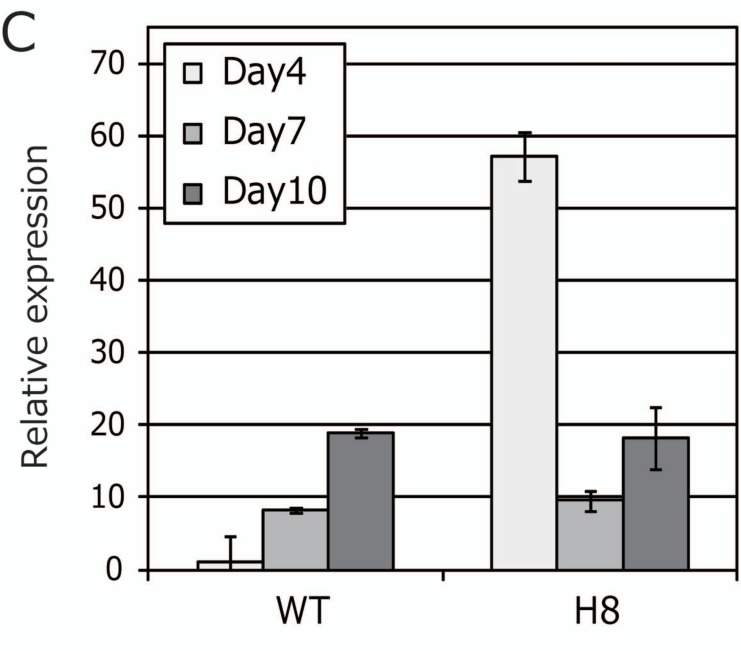
C
70
60
50
40
30
20
10
0
Relative expression
Day4
Day7
Day10
WT
H8

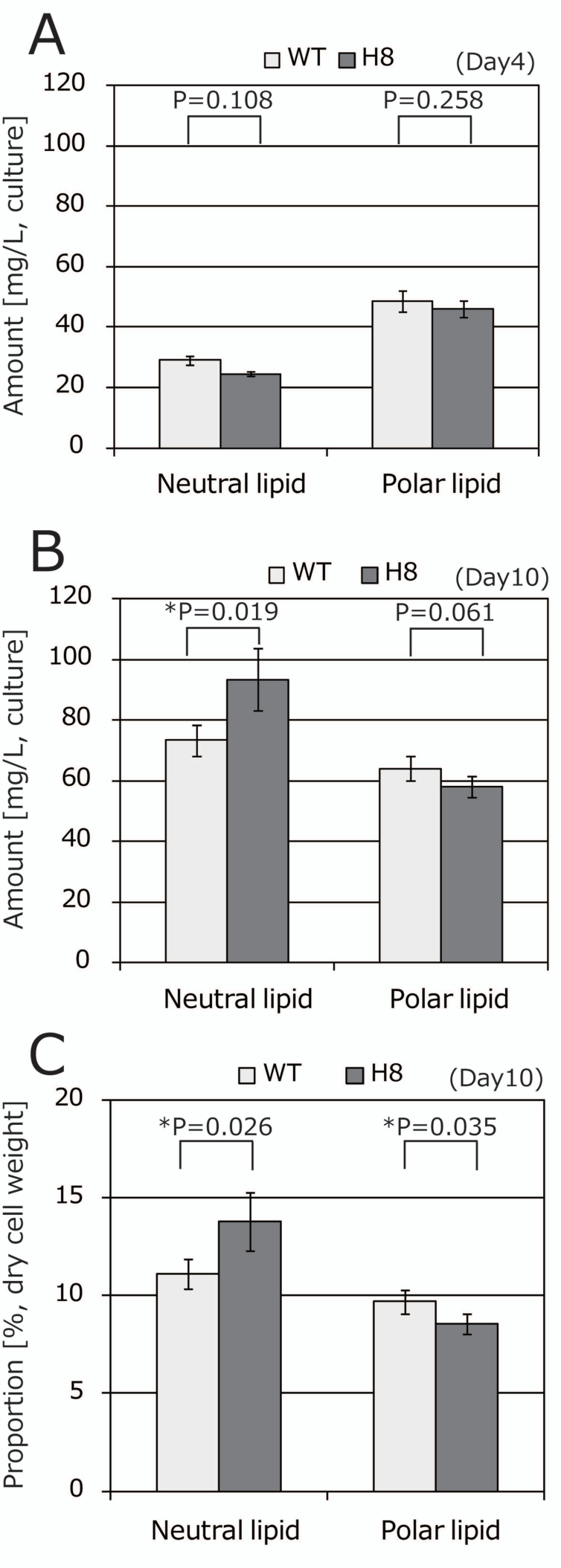
A
WT
H8
(Day4)
P=0.108
P=0.258
Amount [mg/L, culture]
120
100
80
60
40
20
0
Neutral lipid
Polar lipid
B
WT
H8
(Day10)
*P=0.019
P=0.061
Amount [mg/L, culture]
120
100
80
60
40
20
0
Neutral lipid
Polar lipid
C
WT
H8
(Day10)
*P=0.026
*P=0.035
Proportion [%, dry cell weight]
20
15
10
5
0
Neutral lipid
Polar lipid

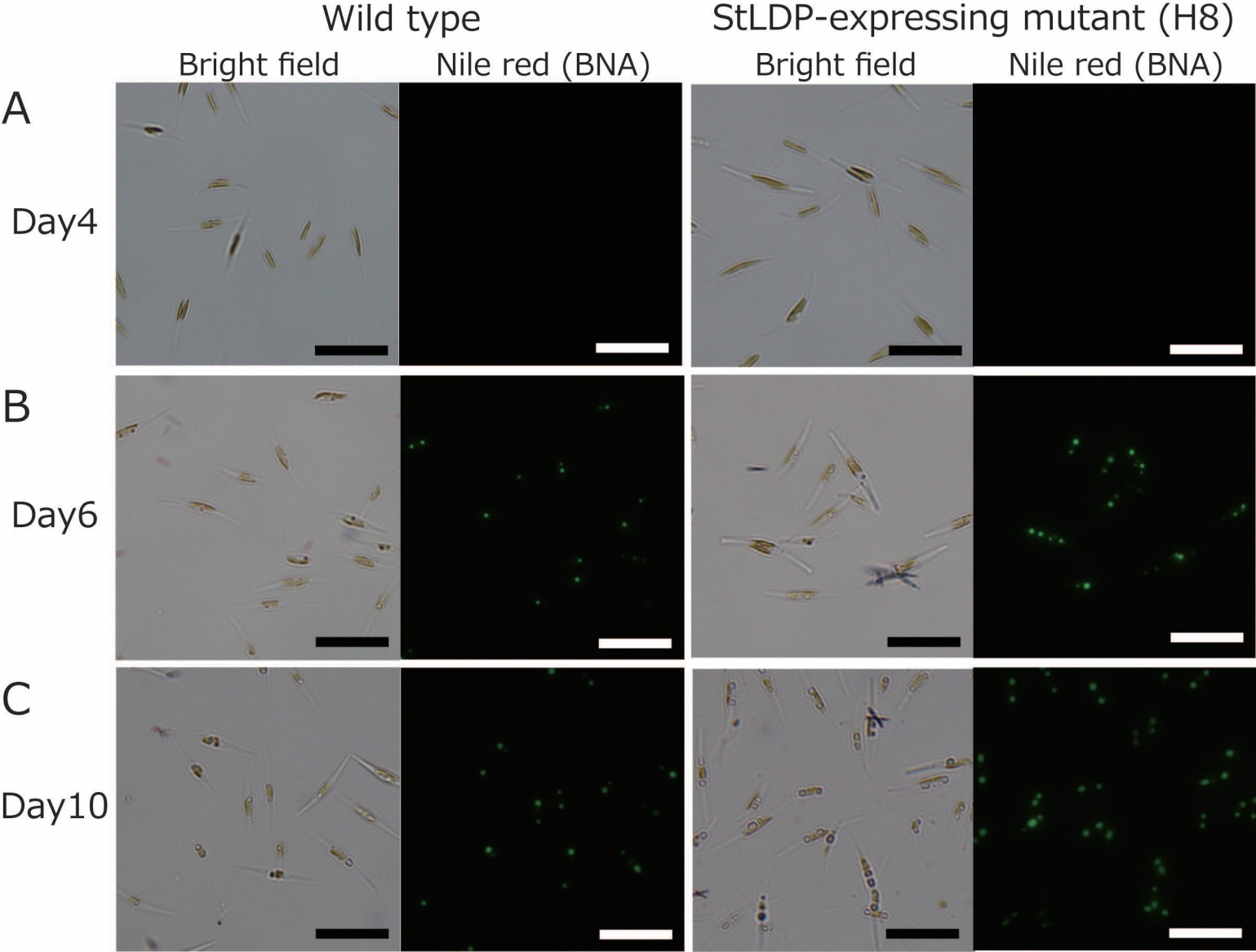
Wild type
StLDP-expressing mutant (H8)
Bright field
Nile red (BNA)
Bright field
Nile red (BNA)
A
Day4
B
Day6
C
Day10

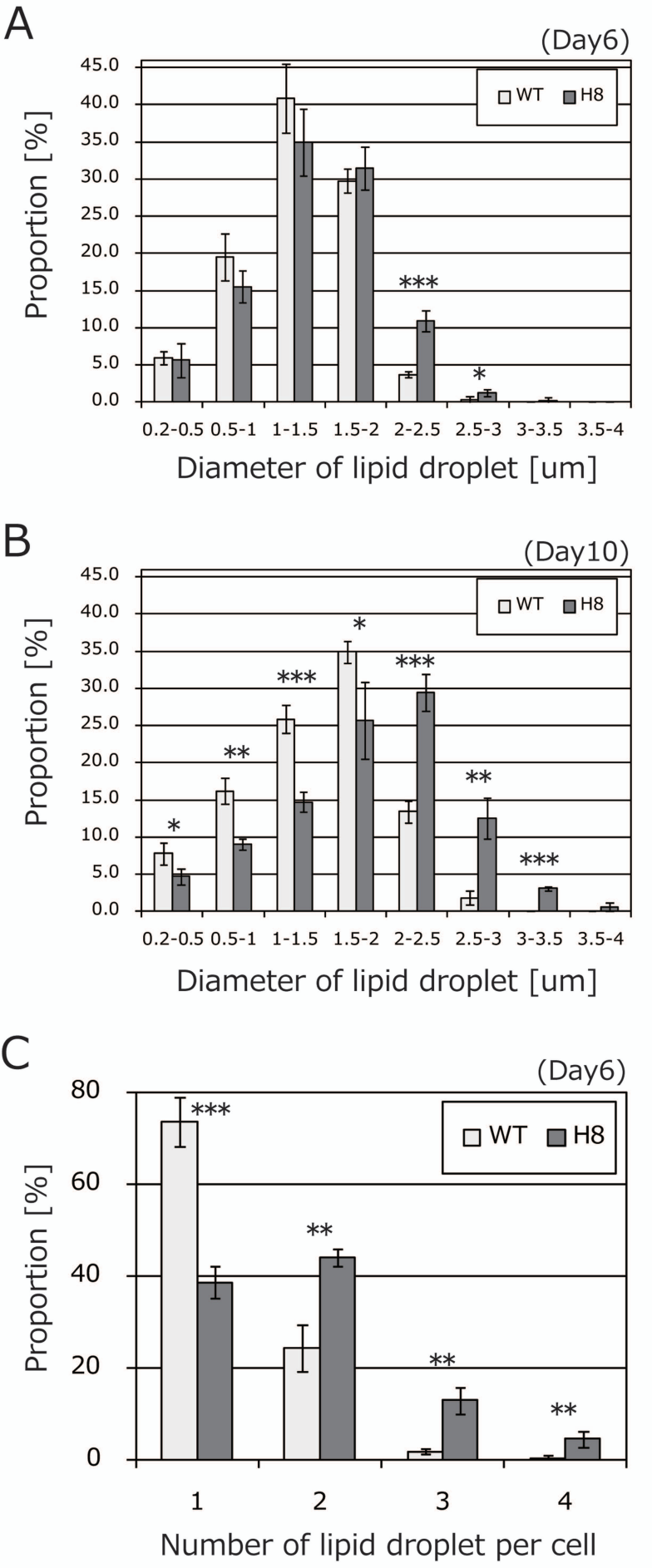
A
(Day6)
WT
H8
Proportion [%]
45.0
40.0
35.0
30.0
25.0
20.0
15.0
10.0
5.0
0.0
***
*
0.2-0.5
0.5-1
1-1.5
1.5-2
2-2.5
2.5-3
3-3.5
3.5-4
Diameter of lipid droplet [um]
B
(Day10)
WT
H8
Proportion [%]
45.0
40.0
35.0
30.0
25.0
20.0
15.0
10.0
5.0
0.0
*
**
***
*
***
**
***
0.2-0.5
0.5-1
1-1.5
1.5-2
2-2.5
2.5-3
3-3.5
3.5-4
Diameter of lipid droplet [um]
C
(Day6)
WT
H8
Proportion [%]
80
60
40
20
0
***
**
**
**
1
2
3
4
Number of lipid droplet per cell

Supplementary Data

Supplementary Table S1. Primers used in this study.

Primer name	Sequence
LD_F	5’-CGAGAATTCATGCCTTCTTCGAGCAATCC-3’
FP-LD_R	5’-CCTCGCCCTTGCTCACTCCACCTCCGCCTCCGCTTGCAGGAACAAGCAT-3’
FP-EGFP_F	5’-GCTTGTTCCTGCAAGCGGAGGCGGAGGTGGAGTGAGCAAGGGCGAGGAG-3’
EGFP_R	5’-CTGAAGCTTTTACTTGTACAGCTCGTCCA-3’
LD-His_R	5’-CTGAAGCTTTTAGTGATGGTGGTGATGGTGGCTTGCAGGAACAAGCATGG-3’
6His-spe_R	5’-TTAGTGATGGTGGTGATGGTG-3’